REPORT DOCUMENTATION PAGE

Form Approved
OMB No. 0704-0188

1. REPORT DATE *(DD-MM-YYYY)*	2. REPORT TYPE	3. DATES COVERED *(From - To)*
18-02-2015	FINAL	1-OCT-11 - 31-DEC-14

4. TITLE AND SUBTITLE
Modeling of Cavitating Flow through Waterjet Propulsors

5a. CONTRACT NUMBER

5b. GRANT NUMBER
N00014-12-1-0197

5c. PROGRAM ELEMENT NUMBER

6. AUTHOR(S)
Jules W. Lindau

5d. PROJECT NUMBER

5e. TASK NUMBER

5f. WORK UNIT NUMBER

7. PERFORMING ORGANIZATION NAME(S) AND ADDRESS(ES)
The Pennsylvania State University Applied Research Labotatory
Office of Sponsored Programs
110 Technology Center Building
University Park, PA 16802-7000

8. PERFORMING ORGANIZATION REPORT NUMBER

9. SPONSORING/MONITORING AGENCY NAME(S) AND ADDRESS(ES)
Office of Naval Research
230 SOUTH DEARBORN
ROOM 380
CHICAGO, IL 60604-1595

10. SPONSOR/MONITOR'S ACRONYM(S)
ONR

11. SPONSORING/MONITORING AGENCY REPORT NUMBER

12. DISTRIBUTION AVAILABILITY STATEMENT
Unlimited

13. SUPPLEMENTARY NOTES

14. ABSTRACT
An axial flow waterjet in water tunnel test configuration has been modeled using both fully un-steady full annulus modeling and a powering iteration methodology. The unsteady results are promising but require more integration and investigation before strong conclusions regarding any un-steady phenomenon may be drawn.

15. SUBJECT TERMS

16. SECURITY CLASSIFICATION OF:			17. LIMITATION OF ABSTRACT	18. NUMBER OF PAGES	19a. NAME OF RESPONSIBLE PERSON
a. REPORT	b. ABSTRACT	c. THIS PAGE	SAR	9	Jules W. Lindau
U	U	U			19b. TELEPONE NUMBER (*Include area code*) 814-865-8938

Modeling of Cavitating Flow through Waterjet Propulsors

Jules W. Lindau

The Pennsylvania State University, Applied Research Laboratory, State College, PA, 16804

1 INTRODUCTION

Axial flow waterjets are a marine propulsion configuration promising to provide a balance between robustness and performance particularly suited to high-speed craft. Due to the contained, internal nature, they may be attractive from a modular vehicle design standpoint. Of course, to achieve performance, they must be integrated with a well-designed inlet, nozzle, and conformal hull. Due to their internal flow nature, waterjets are expected to maintain resistance to cavitation, are amenable to advanced concepts such as thrust vectoring, should exhibit a wide range of nominally high efficiency, and may hypothetically be implemented in all types of surface and submerged marine vehicles. Seemingly, for surface craft, only the inlet must be submerged. However, cavitation and other considerations may drive duct placement as well.

The flow fields through a waterjet propulsor are, however, inherently unsteady and three-dimensional. Furthermore, all ducted propulsors, such as waterjets, are influenced by numerous interacting shear flows. Relative to flow around open propellers, the effects of hub and drive shaft, ducting and shroud, tip gap, and rotor-stator blade row interaction tend to increase flowpath complexity, and decrease peak efficiency. Thus, it is surmised that ducted propulsor performance is more strongly influenced by shear flows, inherent unsteadiness, and interacting vortical structures than open propellers.

For all marine propulsors, cavitation due to local pressure depressions is a persistent condition of interest. Typically, cavitation is a limiting condition on propulsor performance. This may be due to an absolute level of loading that may not be exceeded, resulting in a limit on thrust, i.e., thrust breakdown.

Cavitation breakdown, i.e. the significant alteration in propulsor torque or thrust due to cavitation, may coincide with cavitation choking, at least for a ducted turbomachine. Cavitation choking is quite similar in manifestation to gas dynamic choking. Using a simple throttling device such as a nozzle, and given an inlet reservoir at a fixed total pressure and temperature, there is a minimum outlet backpressure beneath which further reduction fails to increase the mass flow through the nozzle. For gas dynamics, the maximum mass flow coincides with sonic flow at the nozzle throat. For cavitation, the maximum mass flow coincides with the onset of cavitation at the nozzle throat. The throat is then at a physical minimum operating pressure. Any attempt to increase flow rate, without increasing the nozzle total pressure, would cause an increase in the amount of vapor at the throat, reducing the effective flow area, and thus increasing the throat mean velocity, an unsustainable condition. This is described by Mishra and Peles (2005); i.e. choking occurs as soon as vapor is present downstream of the nozzle throat. Although they focus on a current research area, microscale nozzles, they point out that the choking event occurs similarly in any size device. A simple description of cavitation choking is also given in Chapter 8 of Brennen (1995).

3 RESULTS

Steady and time-dependent computational results have been obtained for an axial flow waterjet. Experimental data, in the cavitation tunnel, has been documented over a range of single phase and cavitating conditions (Chesnakas et al 2009). The waterjet is computationally modeled in a fashion approximately representative of the cavitation tunnel experiments. In typical water tunnel experiments, to capture cavitation breakdown, the rotational speed and flow rate are held as close to specified values as possible while the absolute test pressure is modulated. In this way, the parametric effect of cavitation number (for a surface craft, free stream speed and suction head) on operation may be investigated while other specific operating conditions are held constant. The operating conditions of interest are a given flow coefficient (i.e., relative blade leading edge flow angle) and Reynolds number. Numerical results were first obtained at single-phase operating conditions at the given flow coefficient and Reynolds number. Subsequently cavitating solutions were found using the initial conditions first obtained at single phase. Both steady and time-accurate computations were executed.

Some computational results presented here are based on solution of a steady form of the governing equations. At limiting conditions of the flow, when steady solution integration fails it is expected that unsteady integration could be applied to further investigate the nature of the flow which itself is expected to be largely unsteady. Unsteadiness is particularly expected when large vaporous regions appear in the solution causing large vortical structures to be shed along with vapor. It is tempting to investigate such large scale cavity unsteadiness, such as has been done by Lindau et al. (2005(2)) using a Detached Eddy Simulation approach. However, it would seem that for rotating machinery, any investigation of flow unsteadiness should include the unsteady rotor-stator interaction. This is expected to require an unsteady solution of all blade passages in the full turbomachine without periodic assumptions.

3.1 AXWJ-2 WATERJET PUMP

An axial flow waterjet pump (AxWJ-2) has been designed, fabricated, and tested by researchers from Johns Hopkins University and the Naval Surface Warfare Center Carderock Division (NSWCCD). Measurements of the total head rise and shaft torque on flow through the pump have been taken at a range of flow conditions through cavitation breakdown (Chesnakas et al 2009). The single phase and cavitating flow through this pump has been computationally modeled. Results are presented here for a single rotor blade passage. For all conditions presented here, the stator row is modeled with body forces and blockage terms. A powering iteration was used to fully couple the axisymmetric tunnel flow, the three-dimensional rotor, and three-dimensional stator computational flows. Thus the correct, mean and integrated effects of test section inlet boundary layers, stator flow turning, stator blockage, and test section outlet diffusion and boundary layers are, for instance, captured on the rotor flow. However, these effects are circumferentially averaged, and only cavitation in the rotor flow passage is modeled.

3.2 MESH AND RESULTS

In Figure 1, the computational grids used to obtain the steady RANS evaluation of the waterjet flow are presented. For this water tunnel configuration, it is assumed that the flow is reasonably assumed to be axisymmetric a short distance upstream and downstream of the waterjet pump. Therefore, to couple the three-dimensional, but steady, and periodic flow about the rotor and the stator, to each other, and to the upstream and downstream tunnel flow, an axisymmetric grid and flow solution is appropriate. Solution on the through-flow grid, Fig. 1(a) provides inflow velocity and outflow pressure profiles to the rotor and stator grids, pictured in Fig. 1(b). In the through-flow grid solution, body forces equal to circumferentially summed forces on the rotor and stator blades are applied. The forces on the rotor and stator blades are found from solution of the three-dimensional periodic flow determined on the computational meshes in Fig. 1(b). In Fig. 1(a), the forces due to the rotor and the stator are applied in the corresponding labeled, outlined regions. The iteration involves successive solution of the flow on the three meshes. After each solution, an update of inflow velocity and outflow pressure profiles (obtained from the through-flow mesh, Fig. 1(a)) and body forces (obtained respectively from the rotor and stator meshes, Fig. 1(b)) is made. The iteration is complete when the updated profiles do not change significantly with successive iterations.

In Figure 2, alongside experimental measurements (EFD) from the NSWCCD 0.9144m (36in) water tunnel, the single-phase computational fluid dynamics (CFD) based performance, in terms of power and head rise coefficient of the modeled AxWJ-2 is given over a range of flow coefficients. The performance is presented in terms of dimensionless flow rate, $Q^*=Q/(nD^3)$, head rise, $H^*=gH/(n^2D^2)$, and power, $P^*=P/(\rho n^2D^5)$. The CFD head-rise results are given using three different measurement locations and integration assumptions. A maximum head rise, based on integrated total pressure (at locations indicated in Fig. 1) is given using close proximity integration surfaces. A fully integrated head rise based on surfaces at the correct water tunnel measurement locations is also given. Finally, a constant velocity profile (i.e., slug flow) assumption based head rise also using the correct water tunnel pressure measurement locations is given. Note that computed performance based on the appropriate measurement locations, with slug flow assumptions, yields computed head rise and power both in excellent agreement with the EFD. Clearly, the non-isentropic effect of mixing is evident in the CFD and measured water tunnel results. The computed head rise was quite sensitive to the chosen CFD measurement locations (indicated in Fig. 1). The quoted physical measurements were based on tunnel wall static pressure taps and slug flow assumptions. Thus, similar assumptions must be made for purposes of comparison to the tunnel testing when head rise is estimated from the CFD. These results and understandings of the water tunnel measurement procedures were aided by guidance from NSWCCD researchers. Finally, note that at low flow rates and high blade loading conditions, outside

the range of performance reported in Chesnakas et al (2009), the computed flow appears to break down due to massive suction side flow separation (stall).

In Figure 3, photographs from tunnel testing and computed results are shown. The figure illustrates the cavitating flow initiated at the leading edge and in the tip-gap flow over the rotor. It also highlights the overset meshing applied with the intent of better capturing the tip-gap flow. As is evident from the figure, the added overset mesh resolution did not result in significantly different flow solution. In fact, even though the overset mesh involved approximately 500,000 additional cells, the results in terms of cavity size and shape, head rise, and power, was indistinguishable, by any significant measure, between the two cases.

In Figure 4, a series of solutions on a series of computational meshes is shown. This serves to demonstrate grid convergence and the effect of mesh resolution on cavity size shape and features. This solution employs a standard unsteady Reynolds-Averaged Navier-Stokes approach. In Figure 5, an illustration of a CFD solution employing a cavitation model and Delayed Detached Eddy Simulation (Spalart 2009) is presented. This solution utilizes grid (c) of Figure 4. Note the improved resolution of the tip/shroud region cavitation due to the added turbulence simulation. This improved capture of vertical structure supports the notion that some type of eddy simulation along with enhanced mesh resolution will lead to capture of precursor or indicator structures associated with cavitation thrust breakdown.

4 CONCLUSIONS

An axial flow waterjet in water tunnel test configuration has been modeled using both fully unsteady full annulus modeling and a powering iteration methodology. The unsteady results are promising but require more integration and investigation before strong conclusions regarding any unsteady phenomenon may be drawn.

REFERENCES

Abdol-Hamid, K. S. Lakshmanan, B. Carlson, J. R. (1995). 'Application of Navier-Stokes Code PAB3D with k-e Turbulence Model to Attached and Separated Flows' NASA Technical Paper **3480**, NASA Langley Research Center, Hampton, Virginia.

Athavale, M.M. Li, H.Y. Jiang, Y. & Singhal, A.K. (2002) 'Application of the Full Cavitation Model to Pumps and Inducers,' International Journal of Rotating Machinery, **8**(1), pp. 45-56.

Brennen, C. E., (1995). Cavitation and Bubble Dynamics, Chapter 8, *Free Streamline Flows*, Oxford University Press, New York

Chesnakas, C. J. Donnelly, M. J. Pfitsch, D. W., Becnel, A. J. & Schroeder, S. D. (2009). 'Performance Evaluation of the ONR Axial Waterjet 2 (AxWJ-2)'. Hydromechanics Department Report **2009**(089), Carderock Division, Naval Surface Warfare Center.

Coutier-Delgosha, O. Fortes-Patella, R. & Reboud, J.L. (2003) 'Evaluation of the Turbulence Model Influence on the Numerical Simulations of Unsteady Cavitation,' Journal of Fluids Engineering, **125**, pp 38-45.

Kinzel, M. P., Lindau, J. W., Kunz, R. F. & Peltier, L. J. (2007). 'Detached Eddy Simulations for Cavitating Flows'. 18th Computational Fluid Dynamics Conference, Miami, FL, United States.

Kunz, R. F., Boger, D. A., Stinebring, D. R. Chyczewski, T. S., Lindau, J. W., Gibeling, H. J., Venkateswaran, S., & Govindan, T. R. (2000). 'A Preconditioned Navier-Stokes Method for Two-Phase Flows with Application to Cavitation Predication'. Computers and Fluids **29**, pp. 849-875.

Lindau, J. W., Boger, D. A., Medvitz, R. B. & Kunz, R. F. (2005(1)). 'Propeller Cavitation Breakdown Analysis', Journal of Fluids Engineering **127**, pp. 995-1002.

Lindau, J. W., Moody, W. L., Kinzel, M. P. ,Dreyer, J. J., Kunz, R. F. & Paterson, E. G. (2009). 'Computation of Cavitating Flow through Marine Propulsors'. First International Symposium on Marine Propulsors, Trondheim, Norway.

Lindau, J. W., Venkateswaran, S., Kunz, R. F. &. Merkle, C. L. (2001). 'Development of a Fully-Compressible Multiphase Reynolds-Averaged Navier-Stokes Model'. 15th AIAA Computational Fluid Dynamics Conference, Anaheim, California, United States.

Lindau, J.W. Kunz, R.F. Sankaran, V. Stinebring, D.R. & Peltier, L.J. (2005(2)) ,Development and Application of Turbulent, Multiphase CFD to Supercavitation,' 2nd International Symposium on Seawater Drag Reduction, Busan, Korea, 23-26 May.

Merkle, C. L., Feng, J. Z. & Buelow, P. E. O. (1998). 'Computational Modeling of the Dynamics of Sheet Cavitation'. 3rd International Symposium on Cavitation, Grenoble, France.

Mejre, I. Bakir, F. & Rey, R. (2006) 'Comparison of Computational Results Obtained from a Homogeneous Cavitation Model with Experimental Investigations of Three Inducers,' Journal of Fluids Engineering **128**, pp. 1308-1323.

Mishra C. & Peles, Y. (2005) 'Cavitation in flow through a micro-orifice inside a silicon microchannel,' Phys. Fluids 17(013601)

Morgut, M. & Nobile, E. (2011) 'Influence of the Mass Transfer Model on the Numerical Prediction of the Cavitating Flow Around a Marine Propeller,' Second International Symposium on Marine Propulsors, Hamburg, Germany, June.

Schnerr, G.H. Sezal, I.H. & Schmidt, S.J. (2008) 'Numerical Investigation of Three-Dimensional Cloud Cavitation with Special Emphasis on Collapse Induced Shock Dynamics,' Physics of Fluids, **20**(04073).

Schroeder, S. Kim. S.E. & Jasak, H. (2009) 'Toward Predicting Performance of an Axial Flow Waterjet Including the Effects of Cavitation and Thrust Breakdown,' First International Symposium on Marine Propulsors, Trondheim, Norway.

Shih, T. S., Povinelli, L. A., Liu N. S., Potapczuk, M.G. & Lumley, J. T. (1999). 'A Generalized Wall Function'. NASA TM 1999-209398, Glenn Research Center, Cleveland, Ohio.

Singhal, A. K., Athavale M. M., Li, H. & Jiang, Y. (2002). 'Mathematical Basis and Validation of the Full Cavitation Model'. Journal of Fluids Engineering **124**(3), pp. 617 - 624, September.

Spalart, P.R. *Detached-Eddy Simulation*, Annual Review of Fluid Mechanics, vol. 41, pg. 181-202, 2009.

Venkateswaran, S., Lindau, J. W., Kunz, R. F. & Merkle, C. L. (2002). 'Computation of Multiphase Mixture Flows with Compressibility Effects'. Journal of Computational Physics **180**, pp. 54-77.

Venkateswaran, S. & Merkle, C. L. (1999). 'Analysis of Preconditioning Methods for the Euler and Navier-Stokes Equations'. VKI Lecture Series 1999-03, Von Karman Institute, Rhode-Saint-Genese, Belgium, March.

Wilcox, D. C. (1998). Turbulence Modeling for CFD. DCW Industries, La Canada, California.

Wu, H., Soranna, F., Michael, T., Katz, J. & Jessup, S. (2008). 'Cavitation in the Tip Region of the Rotor Blades Within a Waterjet Pump'. Proceedings of FEDSM2008, ASME Fluids Engineering Conference, Jacksonville, Florida, United States.

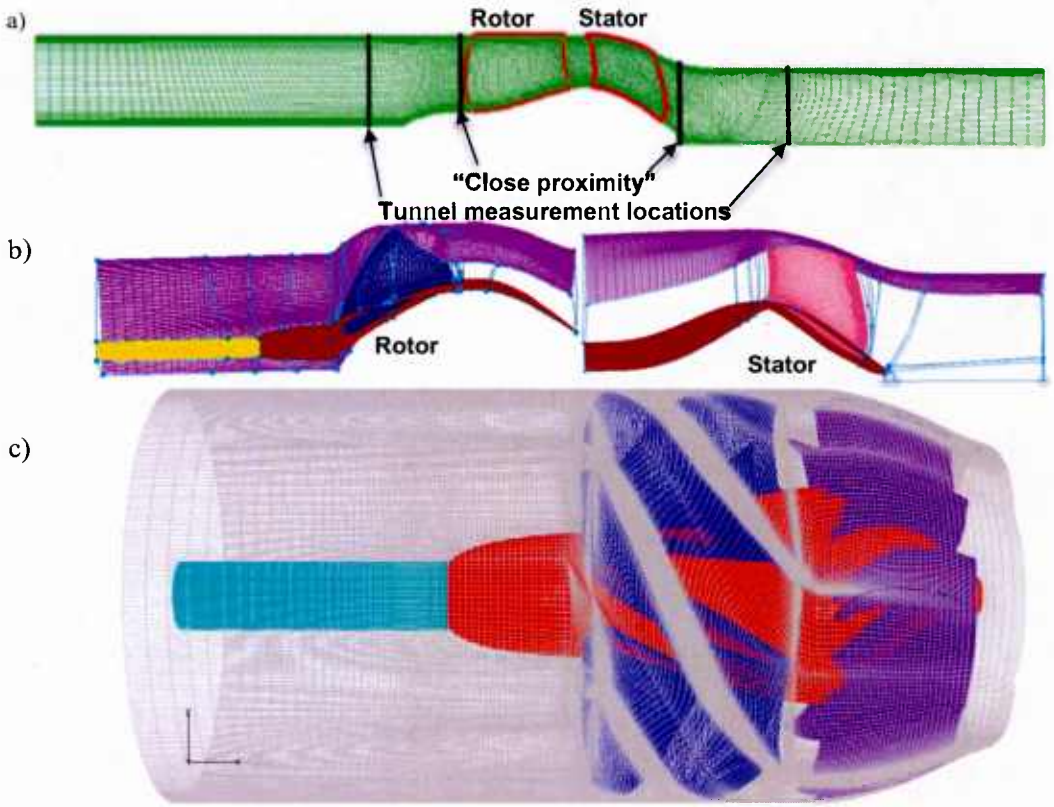

Figure 1: Waterjet pump, AxWJ-2, computational grids shown on all solid surfaces.
a) Axisymmetric through-flow grids with "measurement" locations illustrated.
b) Periodic 3D rotor, and 3D stator grids.
c) 3D grids assembled, repeated, and overlaid for illustration. In part (c), shaft is light blue, hub is red, rotor blades are dark blue, stator blades are purple, and shroud/duct is gray.

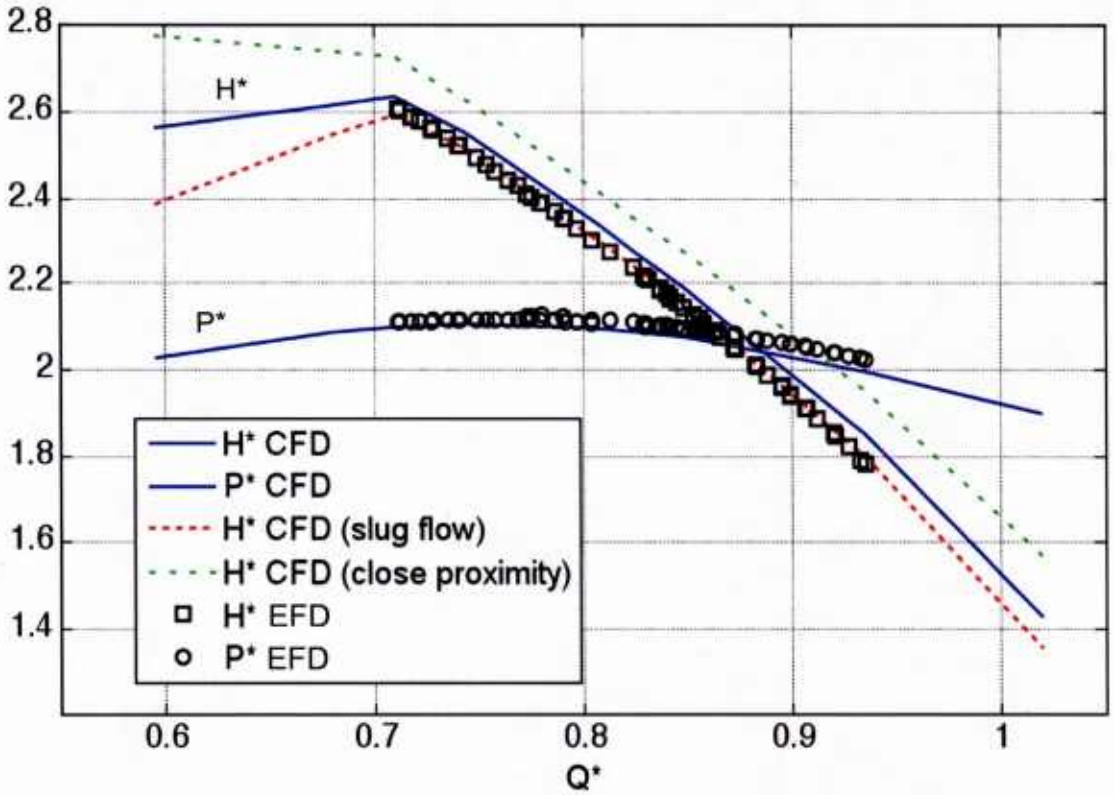

Figure 2: Single-phase flow. Waterjet pump, AxWJ-2, powering iteration integrated results. Dimensionless power [$P^*=(\text{Power})/(\rho n^3 D^5)$] and head rise [$H^*=gH/(\rho n^2 D^2)$] vs. flow rate [$Q^*=Q/(nD^3)$].

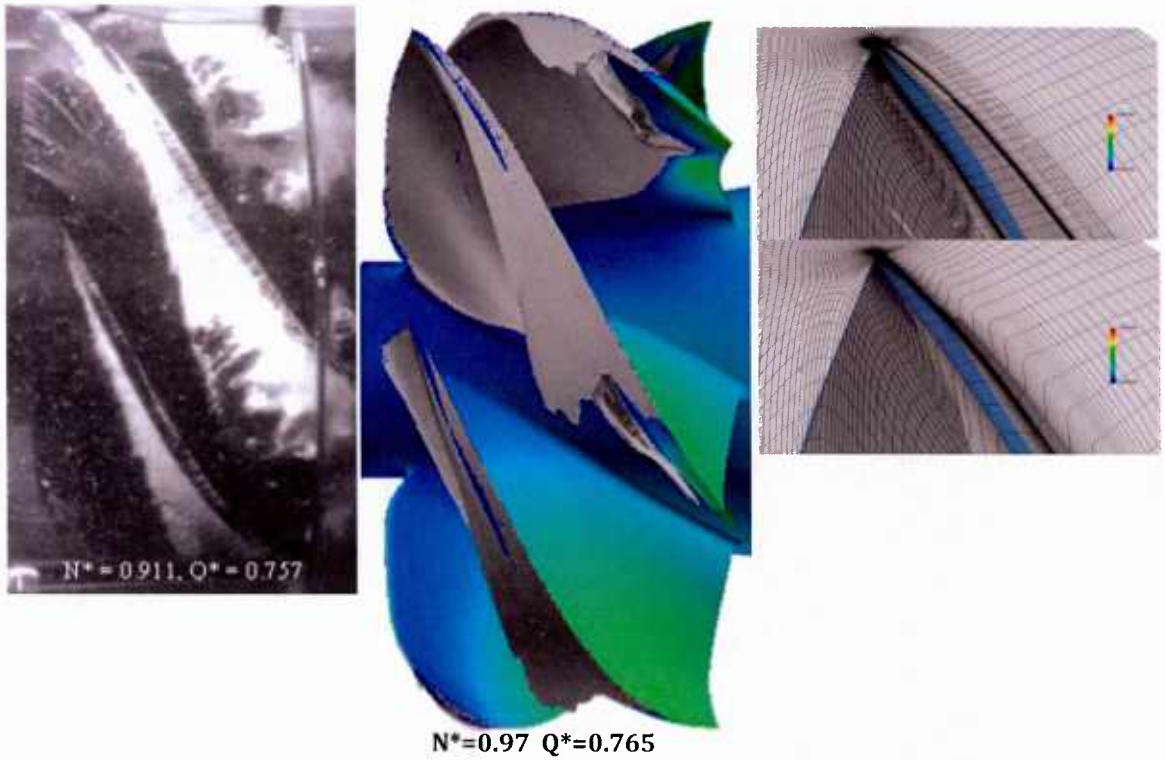

Figure 3: Photograph capturing tip-gap and leading-edge cavitation from waterjet testing and images from steady CFD solutions with and without added tip-gap resolution.

Figure 4: Sensitivity of unsteady cavity resolution to computational mesh. Solution (d) is still evolving.

a) *Coarse* mesh, with converged cavity size and shape shown.

b) *Medium* mesh with uniform refinement of (a) on both rotor and stator blades.

c) *Fine* mesh on rotor tip region but mesh (a) resolution elsewhere.

d) *Extra fine* mesh on rotor volume and tip region mesh (a) resolution of stator.

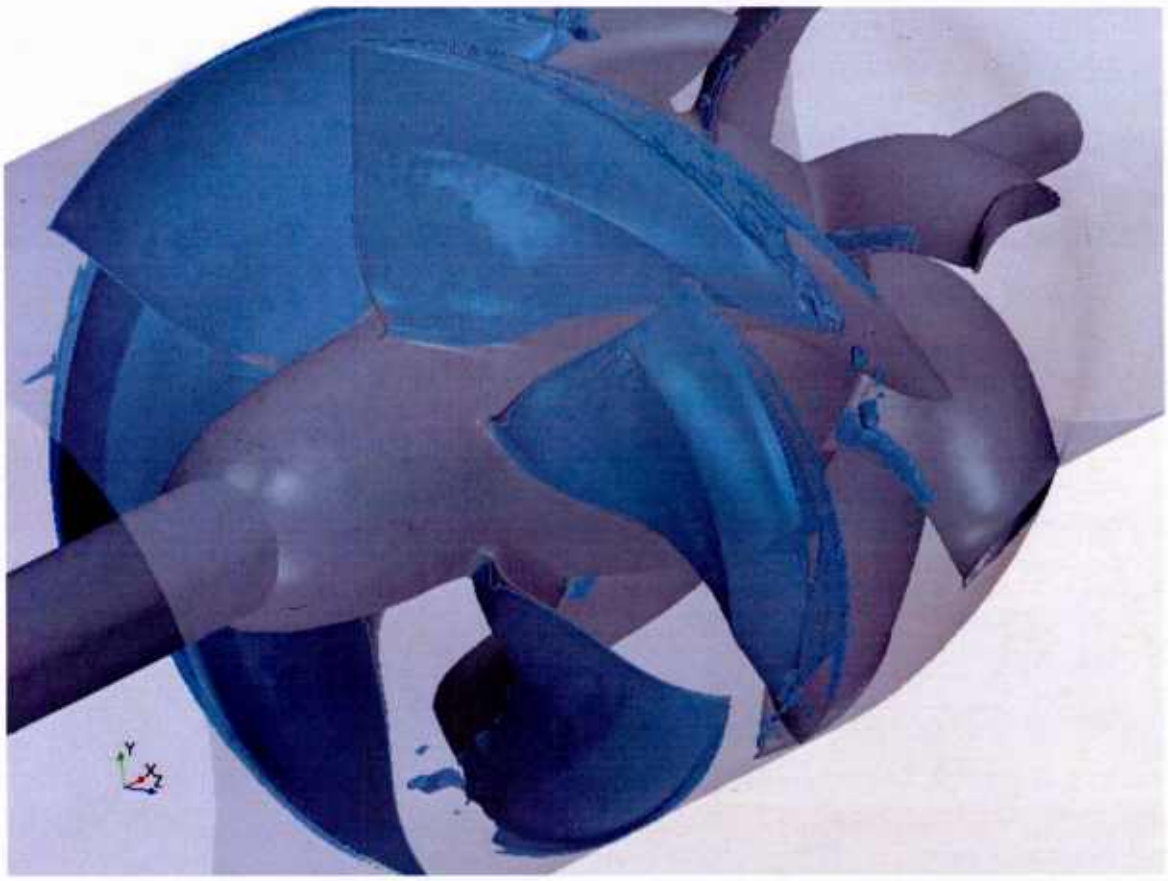

Figure 5: Illustration of detached eddy simulation based solution.